International Journal of Engineering & Technology, 7 (4) (2018) 3843-3846

International Journal of Engineering & Technology

Website: www.sciencepubco.com/index.php/IJET
doi: 10.14419/ijet. v7i4.19396
Research paper

Feasibility of spectral analysis techniques for disruption analysis in Aditya tokamak

T. Thaj Mary Delsy [1] *, N. M. Nandhitha [2], B. Sheela Rani [3]

[1] Research Scholar Sathyabama Institute of Science and Technology, Chennai
[2] Professor Sathyabama Institute of Science and Technology, Chennai
[3] Director Research, Sathyabama Institute of Science and Technology, Chennai
**Corresponding author E-mail: delsykennedy@gmail.com*

Abstract

Aditya Tokamak is a medium size fusion reactor that uses plasma for the generation of power. Magnetic fields are used to confine plasma inside the torus. Release of plasma from its confinement is called plasma disruption. Plasma disruption is a dangerous event, which damages the in – vessel components of the Tokamak. So the early stage prediction of plasma disruption is quite important. Wavelet transform is a powerful tool for the analysis of the non - stationary signals. In this paper, analysis of plasma disruption signals using Biorthogonal wavelet transforms is perform to identify disruption. Plasma current, Vloop, Halpha, Hard X ray, Mirnov coil signal, Soft X-ray are diagnostic signals. Performance is measured in terms of sensitivity and specificity.

Keywords: *Biorthogonal Wavelet; Tokamak; Diagnostic Signals; Skewness; Sensitivity.*

1. Introduction

Plasma disruption in Aditya Tokamak is measured by means of plasma current, Halpha, Vloop, SXR, HXR and Mirnov coil signals[1]. These signals are non stationary in nature. Considerable research is carried out in this area [2]. Table 1 provides the survey on significant work done in this area.From the detailed literature survey, frequency transform cannot be used for analyzing these signals. Of the various transforms, Discrete Wavelet transform is the best suited transform for the analysis of non-stationary signals [3]. From heuristic analysis, it is found that Biorthogonal wavelets provide higher inter class variance and lesser intra class variance than that of other wavelets [4].
Hence in this paper, Biorthogonal wavelet (2.2) is used for the decomposition of these signals. Signals are decomposed into approximation and detailed co-efficient. These co-efficients are then aggregated using statistical parameters namely skewness, kurtosis and mean [5].

2. Research data base

In order to perform the research work, it is necessary to understand the diagnostic signals acquired from Aditya Tokamak.In this work, an extensive research database is created with 249 signals, out of which 103 are that of disrupted signals and the remaining are good signals. In each case, six diagnostic signals are acquired. In order to have a better understanding on these signals, the diagnostic signals of disruption and non-disruption are shown in the Fig 1-2.
From Fig. 1 and 2, following conclusions are made. Significant amplitude in plasma current even after 70 ms, indicates a normal case. In case of disruption, plasma current reaches zero even before 70 ms. Also a burst in Mirnov coil current, positive peak in Halpha and negative loop voltage support the fact that there is a disruption. Hence an efficient signal analysis technique is necessary to indicate these variations in automated signal analysis.

Table 1: Literature Survey on Wavelet Transform Methods

Author /Title of the paper / Journal name/ year/ volume no. / pp	Problem definition	Methodology
Xiaojiao Chen et.al/ Design on the Real-Time Wavelet Filter for ITER PF AC/DC Converter Control / IEEE Transactions On Plasma Science/ JULY 2016/ VOL. 44, NO. 7, pp. 1178-1186.	To reduce the impact of regradation of noise on the control precision of the poloidal field of International Thermonuclear Experimental Reactor.	Daubechies wavelet is used for noise removal.
B.B.S.Kumar et.al / Analysis Using Biorthogonal Wavelet / International Journal Of Innovative Research & Development / June, 2013/ Vol 2/ Issue 6 pp.545-565.	To develop wavelet based techniques for image compression.	Discrete Wavelet Transform is used to obtain a sparse matrix.
H.O.Mota et.al/ A real-time processing system for denoising of partial discharge signals using the wavelet transform/ IEEE Transactions/ 2008/ pp-391-395	To develop Discrete Wavelet Transform(DWT) for denoising the partial discharge signals	Border distortion is removed by using DWT.

3. Statistical wavelet analysis

Biorthogonal wavelet 2.2 is used for decomposing the diagnostic signal into approximation and detailed co-efficients. Statistical parameters namely skewness, kurtosis and mean are obtained on the approximation co-efficients. Skewness measures the alignment of the signal across the mean. Kurtosis is the measure of the flatness

Copyright © 2018 T. Thaj Mary Delsy et. al. This is an open access article distributed under the Creative Commons Attribution License, which permits unrestricted use, distribution, and reproduction in any medium, provided the original work is properly cited.

of the signal, while mean measures the amplitude of the signal. Block diagram of the proposed work is shown in Figure 3.

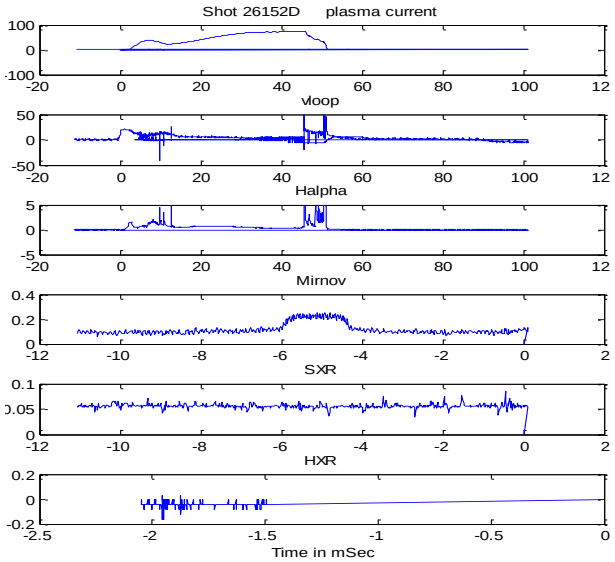


Fig. 1: Representation of the Diagnostic Disruption Signal.

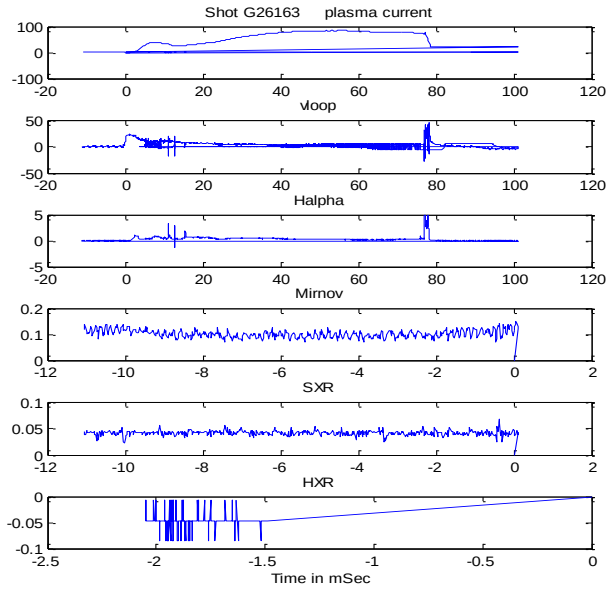


Fig. 2: Representation of the Diagnostic Non-Disruption Signal.

Table 2: Statistical Parameters of the Plasma Current

Sl.no	Shot no	Statistical Parameters (Plasma Current)		
		m1	s1	k1
1	26152D	0.18	23.89	601.64
2	26153D	0.12	21.46	540.79
3	26154D	0.13	19.25	459.86
4	26155D	0.23	20.28	449.13
5	26156D	0.18	21.53	499.61
6	26161D	0.14	19.3	463.35
7	26164D	0.13	24.24	675.37
8	26168D	0.17	25	673.51
9	26170D	0.1	26.2	723.98
10	26177D	0.3	19.21	392.38
11	26179D	0.17	22.87	551.59
12	26180D	0.21	20.32	459.16
13	26181D	0.13	23.67	595.26
14	G26329	0.02	13.79	211.79
15	G26330	0.02	13.40	202.94
16	G26331	0.02	13.50	207.42
17	G26332	0.01	12.19	189.92
18	G26336	0.02	14.36	221.66
19	G26341	0.02	13.19	204.44
20	G26347	0.02	14.31	225.40
21	G26348	0.02	13.87	214.85
22	G26373	0.02	12.72	192.21
23	G26375	0.02	13.36	206.56
24	G26381	0.02	13.46	206.83
25	G26395	0.02	12.74	186.33
26	G26397	0.02	13.01	195.08

Table 3: Statistical parameters of the Vloop signal

Sl. no	Shot no	Statistical Parameters (Vloop)		
		m2	s2	k2
1	26152D	0.84	1.78	17.17
2	26153D	0.7	1.95	22.69
3	26154D	0.39	3.19	37.63
4	26155D	1.21	0.85	9.31
5	26156D	0.62	1.34	15.71
6	26161D	0.59	1.29	13.67
7	26164D	0.26	6.04	70.24
8	26168D	0.07	2.72	39.29
9	26170D	0.12	4.73	70.54
10	26177D	0.79	1.03	12.55
11	26179D	0.05	3.4	45.29
12	26180D	0.07	2.84	37.62
13	26181D	-0.01	5.18	66.3
14	G26408	0.17	0.24	3.13
15	G26412	1.09	0.44	8.11
16	G26413	0.68	0.47	7.97
17	G26414	0.83	0.49	7.19
18	G26419	1.05	1.11	16.65
19	G26420	0.14	5.50	84.57
20	G26421	1.05	1.82	19.46
21	G26422	1.51	0.17	7.40
22	G26423	0.82	1.64	19.96
23	G26425	1.19	0.63	7.22
24	G26427	0.95	1.06	12.92
25	G26428	1.03	1.43	13.06
26	G26429	0.99	0.90	13.91

Mean, skewness and kurtosis determined for the approximation coefficients of Plasma current, Halpha, vloop, soft x ray and hard x ray are shown Tables 2-6. From the statistical parameters of the plasma current ,it observe that the mean value >.1, skewness >14 and kurtosis >350 denotes disruption signal. In Vloop skewness >1 and kurtosis >200 represents disruption, however the disruption is cannot predict by the mean. In Halpha mean <.05, Skewness is >10 and kurtosis >200 represents disruption. In HXR the skewness is negative and kurtosis is >190 represents disruption. In SXR skewness is positive and kurtosis is <250 disruptions.

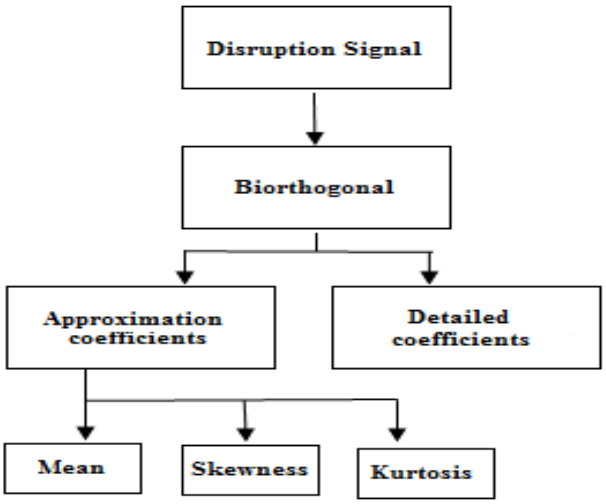


Fig. 3: Block Diagram of Proposed Work.

Table 4: Statistical Parameters of the Halpha Signal

Sl. no	Shot no	Statistical Parameters (Halpha)		
		m3	s3	k3
1	26152D	0.03	16.56	367.52
2	26153D	0.03	16.23	364.96
3	26154D	0.04	14.51	298.87
4	26155D	0.04	13.44	270.03
5	26156D	0.03	14.51	289.73
6	26161D	0.02	22.66	687.25

7	26164D	0.02	17.45	453.1
8	26168D	0.02	22.8	724.94
9	26170D	0.02	18.44	488.68
10	26177D	0.03	14.39	326.62
11	26179D	0.03	15.73	388.43
12	26180D	0.03	16.76	432.67
13	26181D	0.03	16.34	398.45
14	G26331	0.66	5.35	31.12
15	G26332	0.57	5.11	28.01
16	G26336	0.70	5.26	29.38
17	G26341	0.81	5.14	28.27
18	G26347	0.72	4.88	25.86
19	G26348	0.97	4.98	26.57
20	G26373	0.55	5.39	31.12
21	G26375	0.78	4.92	26.31
22	G26381	0.62	5.23	29.53
23	G26395	0.65	5.26	29.66
24	G26397	0.85	4.96	26.07
25	G26399	0.63	5.18	28.67
26	G26400	0.79	4.96	26.26

Table 5: Statistical Parameters of the Disrupted HXR Signal

Sl. No	Shot no	Statistical Parameters (HXR)		
		m5	s5	k5
1	26152D	0	-15.76	290
2	26153D	0	-17.63	395.47
3	26154D	0	-15.39	260.02
4	26155D	0	-14.54	226.32
5	26156D	0	1.23	1361.1
6	26161D	0	-15.26	255.69
7	26164D	0	-14.12	209.98
8	26168D	0	-14.74	234.68
9	26170D	0	-15.05	249.62
10	26177D	0	-17.58	400.81
11	26179D	0	-15.82	273.16
12	26180D	0	-16.61	303.44
13	26181D	0	-13.83	199.33
14	G26397	0	13.56	185.93
15	G26399	0	13.63	188.50
16	G26400	0	13.55	185.44
17	G26402	0	13.54	185.43
18	G26404	0	13.55	185.54
19	G26408	0	13.62	187.98
20	G26412	0	13.56	186.01
21	G26413	0	13.60	187.50
22	G26414	0	13.58	186.77
23	G26419	0	13.57	186.39
24	G26420	0	13.57	186.26
25	G26421	0	13.58	186.69
26	G26422	0	13.58	186.69

Table 6: Statistical Parameters of the SXR Signal

Sl. no	Shot no	Statistical Parameters (SXR)		
		m6	s6	k6
1	26152D	0	13.55	185.44
2	26153D	0	13.56	185.81
3	26154D	0	13.55	185.75
4	26155D	0	13.54	185.15
5	26156D	0	13.6	187.36
6	26161D	0	13.65	189.24
7	26164D	0	13.62	188.28
8	26168D	0	13.6	187.19
9	26170D	0	13.59	187.24
10	26177D	0	13.69	190.69
11	26179D	0	13.75	192.96
12	26180D	0	13.8	195.09
13	26181D	0	13.72	191.8
14	G26331	1.12	83.65	9920.60
15	G26332	-0.01	24.69	4080.30
16	G26336	-0.01	-28.54	1125.10
17	G26341	0.01	89.57	12446.00
18	G26347	0.00	88.20	16424.00
19	G26348	-0.02	-26.65	1365.40
20	G26373	0.00	-38.07	3426.90
21	G26375	0.00	-64.67	8551.60
22	G26381	-0.01	28.60	12605.00
23	G26395	-0.01	-40.37	2151.50
24	G26397	-0.01	-48.51	4934.30
25	G26399	0.00	25.22	6861.60
26	G26400	-0.07	-11.54	1278.60

4. Results and discussion

Threshold limits for the classification of disruption and normal signals is shown in Table 7.

Table 7: Ranges of the Statistical Parameter of the Signals

Signal		Threshold Mean	Skewness	Kurtosis
Plasma Current	N	< .1	< 14	< 250
	D	> .1	> 14	> 350
Vloop	N	-	< 1	< 20
	D	-	> 1	> 20
Halpha	N	> .5	< 6	< 80
	D	< .05	> 6	> 200
Mirnov	N	-	-	-
	D	-	> 13	-
HXR	N	-	+ve	< 190
	D	-	-ve	> 190
SXR	N	-	-ve	> 800
	D	-	> 13	< 800

Based on above limits, signals are classified as disruption or normal. Performance is evaluated in terms of True Positive, True Negative, False Positive and False Negative. Table 8 shows the performance of the individual diagnostic signals and the overall performance is shown in Table 9.

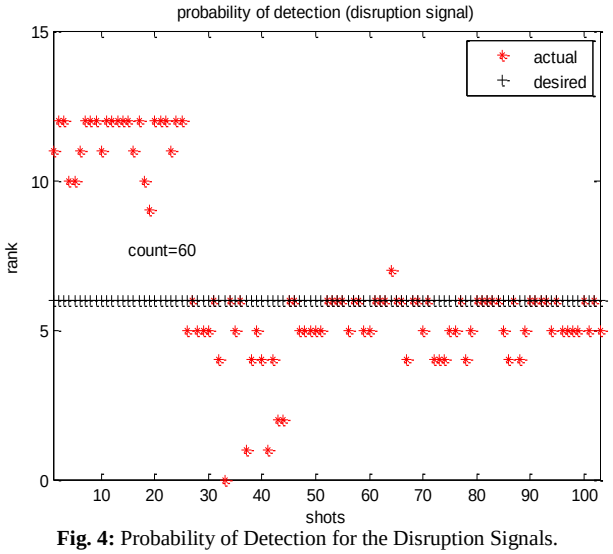


Fig. 4: Probability of Detection for the Disruption Signals.

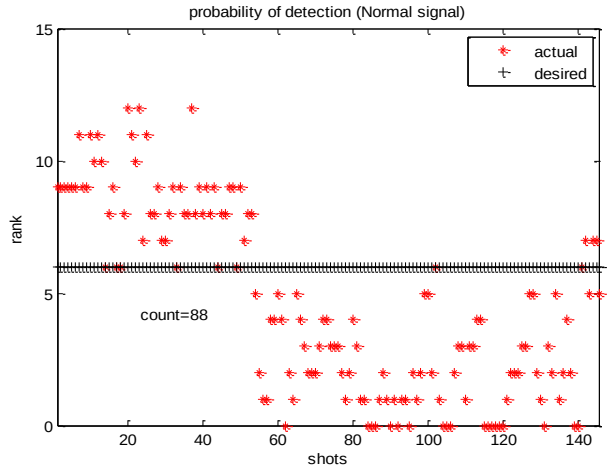


Fig. 5: Probability of Detection for the Normal Signals.

Table 8: Probability of Detection Based on Diagnostic Signals

Signal	Probability	Plasma Current	Vloop	Halpha	HXR	SXR

G as G	True Positive	93	69	90	92	68
G as D	False Negative	53	77	56	54	78
D as D	True Negative	26	97	96	25	30
D as G	False Positive	77	6	7	78	73
sensitivity (%)		63.70	47.26	61.64	63.01	46.58
specificity (%)		25.24	94.17	93.20	24.27	29.13

Table 9: Overall Probability of Detection

Probability	Count
True Positive	88 / 146
False Negative	58 / 146
True Negative	60 / 103
False Positive	43 / 103

From the above Table 9, sensitivity and specificity are 60.27% and 58.25% respectively. And also the predictive value for a positive result (PV+) and a negative result (PV-) are 59.45% and 50.84%.

Fig.4 Probability of detection for the disruption signals

The graphical representation of the Probability of detection of the disruption and normal signals are shown in figure 4 and 5. In total, 12 possible ranks are calculated from the statistical parameters of all the diagnostics signals. The desired rank of disruption is considered as 6. If the rank is greater than 5,then consider as disruption otherwise normal. By this condition fig.4 shows that the probability of detection of disruption is 60 out of 103 signals and normal is 88 out of 146 signals is shown in fig.5

5. Conclusion and future work

In this paper, an automated plasma disruption analysis technique is developed using Discrete Wavelet Transform. Statistical parameters namely mean, skewness and kurtosis are determined on the diagonal co-efficient. Performance is analyzed in terms of true positive, false negative, true negative and false positive. Sensitivity and specificity were also calculated. Sensitivity and specificity are 60.27% and 58.25% respectively. And also the predictive value for a positive result (PV+) and a negative result (PV-) are 59.45% and 50.84%.In order to improve the performance further, it is necessary to identify an appropriate transform.

Acknowledgement

We would like to offer our special thanks to Mr.Rakesh L.Tanna, Scientist & Section head and Mr.Joydeep Ghosh,Scientist & Project Leader, Aditya Tokamak, IPR, Bhat, Gandhinagar, India for their support.

References

[1] Bhooshan Paradkar, J. Ghosh, P. K. Chattopadhyay, R. L. Tanna, D. Raju, S. B. Bhatt, C. V. S. Rao, Sankar Joisa, Santanu Banerjee, R. Manchanda, C. N. Gupta, Y. C. Saxena, *and* Aditya Team, Runaway –loss induced negative and positive loop voltage spikes in the Aditya Tokamak Physics of Plasma, 2010, Vol.17, Issue 9, doi.org/10.1063/1.3474949.

[2] K. Sudheera and N. M. Nandhitha , Application of Hilbert Transform for Flaw Characterization in Ultrasonic Signals, Indian Journal of Science and Technology, , DOI: 10.17485/ijst/2015/v8i13/56303, July 2015, Vol 8(13), pp.1-6 https://doi.org/10.17485/ijst/2015/v8i13/56303.

[3] Jose Albin, A & N.M., Nandhitha, Text independent human voice ranking system for audio search engines using wavelet features, ARPN Journal of Engineering and Applied Sciences, 2015, 10, pp.1650-1653.

[4] T. T. M. Delsy, N. M. Nandhitha, R. L. Tanna and J. Ghosh, "Spectral statistical analysis of low frequency coefficients from diagnostic signals depicting MHD disruptions," *2017 International Conference on Circuit, Power and Computing Technologies (ICCPCT), Kollam,* 2017, 978.- 1- 5090-4967- 7/17/$31.00 © 2017 IEEE. https://doi.org/10.1109/ICCPCT.2017.8074353.

[5] Selvarasu, N & Nachiappan, A & N.M., Nandhitha, Effective representation of Non-Uniformity and asymmetry in breast thermographs using statistical parameters on histograms of Wavelet Coefficients for cancer detection. European Journal of Scientific Research.2012, 80, pp.10-19.

[6] R L Tanna, J Ghosh, Harshita Raj, Rohit Kumar, Suman Aich, Vaibhav Ranjan, K A Jadeja, K M Patel, S B Bhatt, K Sathyanarayana1, Production And Preliminary Results From The Aditya Upgrade Tokamak, Plasma Science and Technology, May 2018 , Vol.20, Number 7.

[7] Binh Nguyen, Dang Nguyen, Wanli Ma, and Dat Tran, Wavelet transform and adaptive arithmetic coding techniques for EEG lossy compression, 978-1-5090-6182-2/17/$31.00 ©2017 IEEE, pp.3153-3160.

[8] Xiaojiao Chen, Liansheng Huang, Peng Fu, Ge Gao, Shiying He, Jun Shen, Lili Zhu, and Lin Dong , 'The Design on the Real-Time Wavelet Filter for ITER PF AC/DC Converter Control System', IEEE Transactions on Plasma Science, Vol. 44, No. 7, 2016, pp1178 - 1186. https://doi.org/10.1109/TPS.2016.2572200.

[9] C. Vimala and P. A. Priya, "Noise reduction based on double density discrete wavelet transform," in Proc. Int. Conf. Smart Struct. Syst. (ICSSS), Oct. 2014, pp. 15–18. https://doi.org/10.1109/ICSSS.2014.7006177.

[10] SE Roslin, NM Nandhitha, CCJ Rekha, A Monisha,Node state information based adaptive power allocation and energy efficient routing using fuzzy logic for wireless sensor network, Int J Appl Eng Res 9 (21), pp.8575-92.

[11] Baochen Jiang, Aiping Yang, Chengyou Wang and Zhengxin Hou, Implementation of Biorthogonal Wavelet Transform Using Discrete Cosine Sequency Filter International Journal of Signal Processing, Image Processing and Pattern Recognition Vol. 6, No. 4, August, 2013, pp 179 – 189.

[12] H. O. Mota, N. D. O. Volpini, G. F. Rodrigues , F. H. Vasconcelos ,A real-time processing system for denoising of partial discharge signals using the wavelet transform, 978-1-4244-2092-6/08/$25.00 ©2008 IEEE,pp 391-395.

[13] K. Yoshimatsu, N. Okamoto, Y. Kawahara, K. Schneider and M. Farge. 'Coherent vorticity and current density simulation of three-dimensional magnetohydrodynamic turbulence using orthogonal wavelets'. Geophysical and Astrophysical Fluid Dynamics, 2013, 107(1-2), pp.73-80. https://doi.org/10.1080/03091929.2012.654790.

[14] B.B.S.Kumar, Dr.P.S.Satyanarayana, 'Image Analysis Using Biorthogonal Wavelet', International Journal Of Innovative Research & Development, June, 2013 Vol 2 Issue 6, pp.543 – 565.

[15] Zhang, H., Blackburn, T. R. et al. "A novel wavelet transform technique for on-line partial discharge measurements – part 1: WT denoising algorithm." IEEE Transactions on Dielectrics and Electrical Insulation. Frebruary 2007 Vol. 14, no. 1.

[16] P. Fu et al., "Review and analysis of the AC/DC converter of ITER coil power supply," in Proc. 25th Annu. IEEE Appl. Power Electron. Conf.Expo. (APEC), Feb. 2010, pp. 1810–1816. https://doi.org/10.1109/APEC.2010.5433479.

[17] R. W. Schafer, "What is a Savitzky–Golay filter?" IEEE Signal Process. Mag., Jul. 2011, Vol. 28, no. 4, pp. 111–117. https://doi.org/10.1109/MSP.2011.941097.

[18] Q. Gao, Y. Lu, D. Sun, and D. Zhang, "A multiscale products technique for denoising of dna capillary electrophoresis signals," Meas. Sci. Technol., 2013, Vol. 24, no. 6, 2013, https://doi.org/10.1088/0957-0233/24/6/065004.

[19] K. Hallatschek and M. Zilker, "Real time data acquisition with transputers and PowerPCs using the wavelet transform for event detection," IEEE Trans. Nucl. Sci., Aug. 1998, Vol. 45, no. 4, pp. 1872–1876. https://doi.org/10.1109/23.710954.

[20] J. Gruber, Z. Sekeresova, J. Hlina, and J. Sonsky, "Analysis of thermal plasma dynamics in 3-D using tomographical reconstruction and wavelet analysis," IEEE Trans. Plasma Sci., Nov. 2011, Vol. 39, no. 11, pp. 2850–2851. https://doi.org/10.1109/TPS.2011.2155093.

[21] Y. Hongwen et al., "On the sequential control of ITER poloidal field converters for reactive power reduction," Plasma Sci. Technol., 2014, Vol. 16, no. 12, p.p.1147. https://doi.org/10.1088/1009-0630/16/12/11.